the FEBS Journal

Polysaccharide binding sites in hyaluronate lyase – crystal structures of native phage–encoded hyaluronate lyase and its complexes with ascorbic acid and lactose

Parul Mishra[1,*], R. Prem Kumar[2,*], Abdul S. Ethayathulla[2], Nagendra Singh[2], Sujata Sharma[2], Markus Perbandt[3], Christian Betzel[3], Punit Kaur[2], Alagiri Srinivasan[2], Vinod Bhakuni[1] and Tej P. Singh[2]

1 Department of Molecular and Structural Biology, Central Drug Research Institute, Lucknow, India
2 Department of Biophysics, All India Institute of Medical Sciences, New Delhi, India
3 Department of Biochemistry and Molecular Biology, University of Hamburg, Germany

Keywords
ascorbic acid complex; hyaluranidase; HylP2; lactose complex; triple-stranded β-helix

Correspondence
T. P. Singh, Department of Biophysics, All India Institute of Medical Sciences, Ansari Nagar, New Delhi 110 029, India
Fax: +91 11 2658 8663
Tel: +91 11 2658 8931
E-mail: tpsingh.aiims@gmail.com

Database
Atomic coordinates have been deposited in the Protein Data Bank as entries 2YW0 (native), 3EKA (ascorbic acid complex) and 2YVV (lactose complex)

*These authors contributed equally to this work

(Received 24 November 2008, revised 11 April 2009, accepted 17 April 2009)

doi:10.1111/j.1742-4658.2009.07065.x

Hyaluronate lyases are a class of endoglycosaminidase enzymes with a high level of complexity and heterogeneity. The main function of the *Streptococcus pyogenes* bacteriophage protein hyaluronate lyase, HylP2, is to degrade hyaluronan into unsaturated disaccharide units. HylP2 was cloned, overexpressed and purified to homogeneity. The recombinant HylP2 exists as a homotrimer with a molecular mass of approximately 110 kDa under physiological conditions. The HylP2 was crystallized and the crystals were soaked in two separate reservoir solutions containing ascorbic acid and lactose, respectively. The crystal structures of native HylP2 and its two complexes with ascorbic acid and lactose have been determined. HylP2 folds into four distinct domains with a central core consisting of 16 antiparallel β-strands forming an irregular triangular tube designated as triple-stranded β-helix. The structures of complexes show that three molecules each of ascorbic acid and lactose bind to protein at the sugar binding groove in the triple-stranded β-helix domain. Both ascorbic acid and lactose molecules occupy almost identical subsites in the long saccharide binding groove. Both ligands are involved in several hydrogen bonded interactions at each subsite. The binding characteristics and stereochemical properties indicate that Tyr264 may be involved in the catalytic activity of HylP2. The mutation of Tyr264 to Phe264 supports this observation.

Hyaluronidases are produced by a variety of organisms, including mammals, insects, leeches and bacteria. Besides these well-known sources, phage-encoded hyaluronidases from *Streptococcus pyogenes* and *Streptococcus equi* have also been identified [1,2]. Functionally, hyaluronidases degrade high molecular weight polysaccharides of the glycosaminoglycans family either by hydrolysis (eukaryotic) or by a β-elimination (bacterial hyaluranidases) mechanism. The bacterial hyaluronidases, better known as lyases, recognize mainly hyaluronic acid (HA) and chondroitin sulfates and, to a smaller extent, dermatan sulfates of the host connective tissue, the degradation of which leads to spreading of the bacterial infection. *S. pyogenes* is an HA-encapsulated group A *Streptococci* that is known to have bacteriophage sequences in its genome [3]. The hyaluronate lyase, HylP2, is the bacteriophage hyaluronidase present in the *S. pyogenes* strain 10403 [4].

Abbreviations
HA, hyaluronic acid; HylP, hyaluronate lyase.

Another hyaluronidase, HylP1, has been isolated and characterized from the prophage sequences of *S. pyogenes* strain SF370.1 [5]. Hyaluronate lyases from various species indicate different specificities towards polysaccharide substrates [6]. These bacteriophage hyaluranidases are lyases, catalyzing through a β-elimination mechanism similar to the bacterial hyaluranidases. As opposed to the bacterial lyases, however, the phage hyaluronidase recognizes hyaluronan as its only substrate [7]. The bound hyaluronidase produced by the bacteriophage is not secreted from the cell and is a part of the bacteriophage particle. Its main function is to assist the phage in the penetration of the HA capsule that surrounds the host cells of this phage and hence gain access to the cell surface of the host *Streptococcus* [4]. Apart from this, an indirect role of the bacteriophage-encoded hyaluronidase in streptococcal disease has also been indicated where it transforms the nonvirulent streptococcal strains into virulent strains. The enzyme, which is not associated with the phage particles, may be involved in degrading HA of the human connective tissue, thereby allowing dissemination of the phage-encoded erythrogenic toxin, which is responsible at least in part for the visible rash in scarlet fever [8].

The crystal structures of three differently organized hyaluronidases have been reported from bee venom, *Streptococcus pneumoniae* and *Streptococcus agalactiae*, which are monomeric proteins with distinct α and β domains. The structure of a group A streptococcal phage-encoded native protein hyaluronate lyase (HylP1) has been described [5]. It is a triple-stranded structure containing three copies of the active centre on the triple fibre itself without the need for any additional accessory catalytic domain. The unusual structural features of HylP1 have been described briefly, although the polysaccharide binding regions and associated structural changes upon ligand binding have not been characterized so far. To understand the structure and function relationship of unusually structured triple-stranded hyaluronate lyases, we have cloned the *S. pyogenes* bacteriophage protein hyaluronate lyase (HylP2) and have shown biochemically that ascorbic acid inhibits the activity of HylP2. We report the detailed crystal structures of native protein HylP2 and two of its complexes with an inhibitor ascorbic acid (Fig. 1A) and a substrate product disaccharide analogue lactose (Fig. 1B). These are the first reports concerning the structures of complexes of hyaluronate lyase with ligands. These structures have revealed considerable detail with respect to the saccharide binding groove in hyaluronate lyase and useful information has been obtained about subsite structures. The amino acid residues involved in the interactions with ligands, as well as those involved in the catalysis, have been identified.

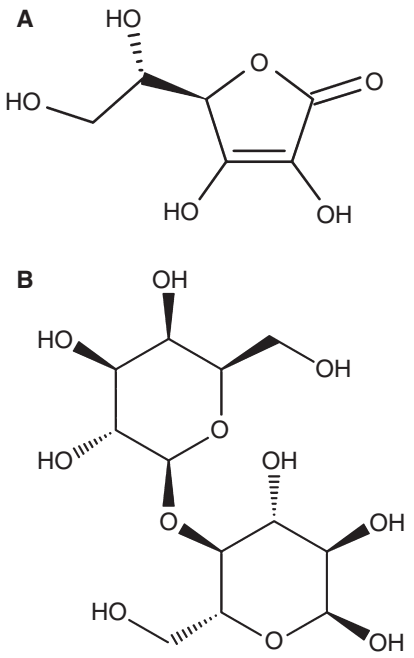

Fig. 1. Chemical structures of (A) ascorbic acid and (B) lactose.

Results

Overall structure

The parameters of refined final models of native protein HylP2 and its two complexes with ascorbic acid and lactose are summarized in Table 1. The polypeptide chain of HylP2 is well defined from residues 7–338. The final $|2F_o - F_c|$ electron density map is continuous and well defined for both the backbone and side chains of the protein. The structure determination revealed excellent electron densities for the ligands, ascorbic acid (Fig. 2) and lactose (Fig. 3), in the respective complex structures. The overall folding of the protein chain of HylP2 (Fig. 4A) is similar to that of HylP1 with an rmsd shift of 0.6 Å for the Cα atoms. The view from the top shows the locations of the two ligands at overlapping positions, which are related by three-fold symmetry (Fig. 4B). All the figures were constructed using PYMOL [9]. The Ramachandran plots for the main chain torsion angles (φ, ψ) [10] of all three structures show that more than 88% of the residues in the native and lactose structures and more than 84% of the residues in the

Table 1. Summary of data collection and refinement statistics.

Parameter	Native	Ascorbic acid	Lactose
Protein Data Bank ID	2YW0	3EKA	2YVV
Data collection			
Space group	H32	H32	H32
Unit cell dimensions (Å)			
a = *b*	58.8	58.5	59.1
c	586.1	583.5	588.8
Number of unique reflections	12713	6874	12827
Resolution range (Å)	50.0–2.6	50.0–3.1	50.0–2.6
Highest resolution shell (Å)	2.64–2.60	3.15–3.10	2.64–2.60
Redundancy[a]	9.7 (9.7)	6.2 (6.2)	8.8 (8.8)
Completeness (%)	99.8 (100.0)	90.0 (92.0)	99.0 (100.0)
R_{sym} (%)	3.8 (32.4)	11.0 (43.4)	6.4 (22.4)
I/σ	6.3 (2.2)	11.7 (2.6)	6.7 (2.3)
Refinement			
R_{cryst} (for all data) (%)[b]	19.1	19.7	19.1
R_{free} (5% data) (%)	21.9	23.3	22.6
Number of non-hydrogen atoms			
Protein	2515	2515	2515
Water	108	68	110
Ligand	–	36	69
rmsd[c]			
Bond lengths (Å)	0.01	0.02	0.01
Bond angles (°)	1.6	2.3	1.6
Dihedral angles (°)	18.2	20.8	18.4
Overall G-factor	0.01	−0.3	0.01
Average B-factor (Å^2)			
All atoms	48.0	51.7	47.1
Protein atoms	48.0	50.8	47.3
Water atoms	47.9	58.5	51.1
Ligand atoms	–	53.1	35.3
From Wilson plot	64.7	69.6	66.9
Ramachandran plot statistics			
Residues in the most favoured regions (%)	88.4	84.3	88.4
Residues in the additionally allowed regions (%)	11.6	15.0	11.6
Residues in the generously allowed regions (%)	–	0.7	–

[a] Values in parentheses refer to the highest resolution shell. [b] $R_{cryst} = \Sigma||F_{obs}| - |F_{calc}||/\Sigma|F_{obs}|$ where F_{obs} and F_{calc} are the observed and calculated structure factors, respectively. [c] Root mean square deviation.

structure of the complex with ascorbic acid are in the most favoured regions, as defined using the software PROCHECK [11]. The N-terminal domain consisting of residues 7–56 adopts a mixed α/β conformation, forming a globular capping. It is followed by a stretch of coiled coils with segmented α-helical regions to residue 108. This is followed by the central core consisting of 16 antiparallel β-strands with flexible loops between strands. This generates an irregular

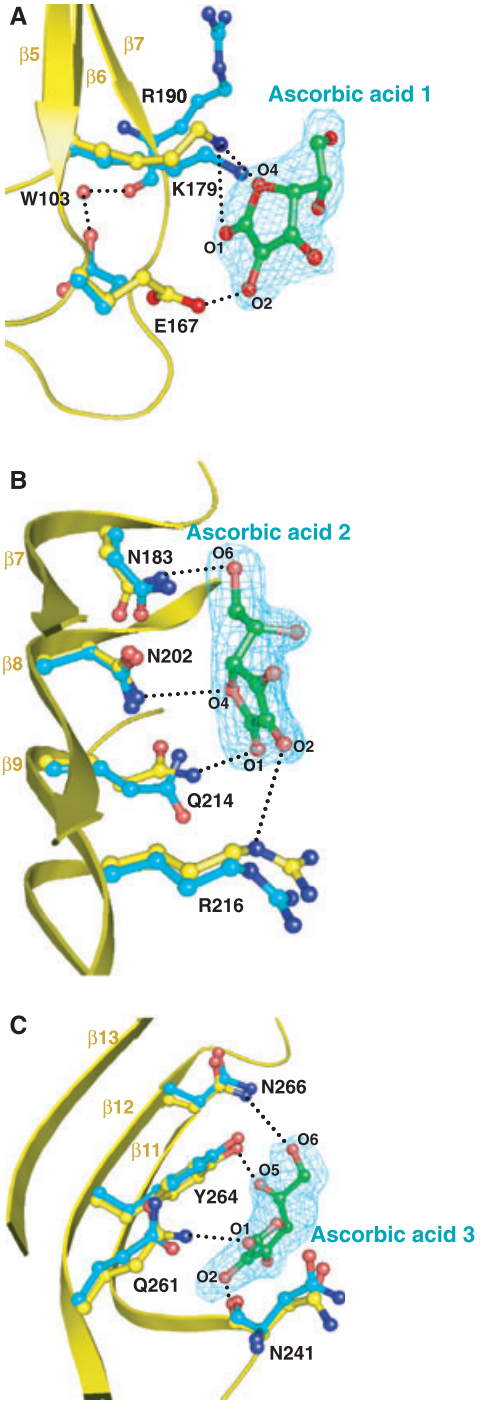

Fig. 2. The difference Fourier ($|F_o - F_c|$) map showing electron densities at a cut-off of 2.0 σ for three ascorbic acid molecules (A), (B) and (C) at three distantly spaced regions of the concave polysaccharide binding site in HylP2. The conformational changes observed in the side chains of Glu167 and Lys179 upon binding to ascorbic acid are shown by superimposing their binding regions of native structure (cyan) and that of complexed structure with ascorbic acid (yellow) at subsites (A), (B) and (C), respectively. The dotted lines indicate hydrogen bonds between protein and ligand atoms.

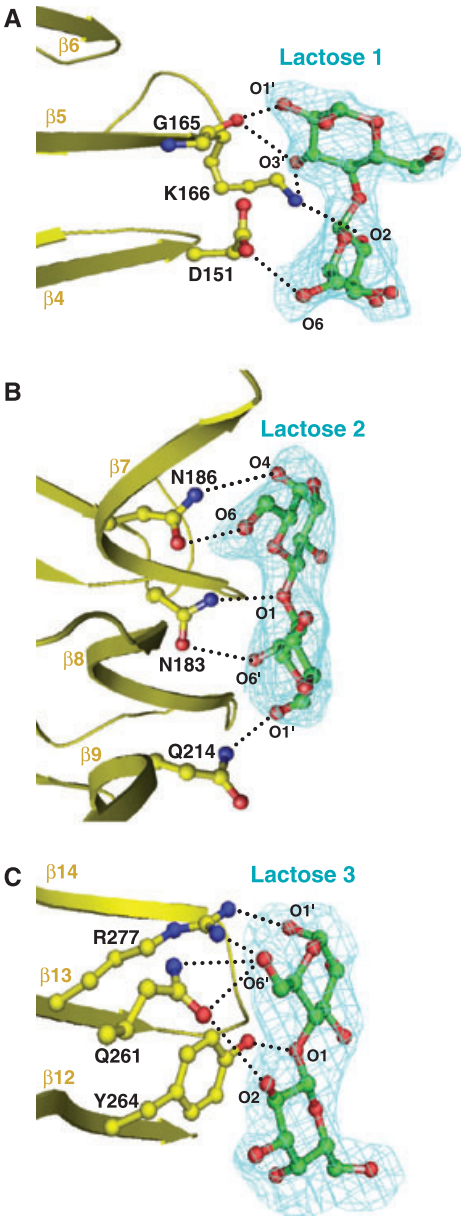

Fig. 3. The difference Fourier ($|F_o - F_c|$) map showing electron densities at a cut-off of 2.0 σ for three lactose molecules (A), (B) and (C) at three distantly spaced regions of the concave polysaccharide binding site in HylP2. The interactions between protein residues and ligand molecules are indicated by dotted lines.

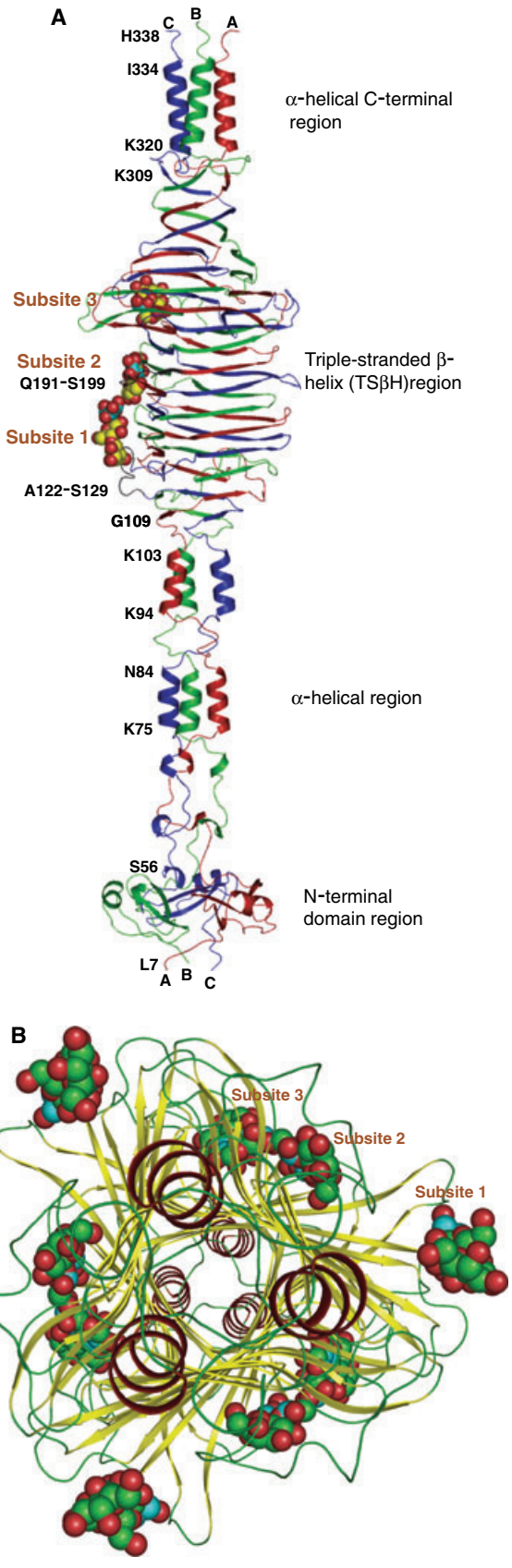

Fig. 4. (A) The 3D structure of HylP2 showing each monomer chain in three different colours. Four different regions are indicated from residues 7–56, 57–108, 109–309 and 320–334. Ascorbic acid and lactose molecule binds at three subsites in the polysaccharide binding site of the TSβH domain of HylP2. The positions of ligands are indicated at the substrate binding groove. (B) The view from the top shows the subsites of ascorbic acid and lactose binding in HylP2.

triangular tube designated as triple-stranded β-helix (TSβH), similar to that reported in HylP1 [5]. This region extends over residues 109–309 and is approximately 80 Å in length. It is separated by a sharp loop (residues 310–319) from the α-helical C-terminal region (residues 320–334). The right-handed TSβH forms a triangular tube where three faces are made by alternating β-strands from each of the polypeptides. The β-strands are orthogonal to the long helical axis. There are three sides on the molecular tube where carbohydrate chains become attached. These sides adopt concave shapes to promote a more specific binding. The activity of the enzyme was shown to be lost in the structure of HylP1 [5] when Asp137 was mutated to Ala137 and Tyr149 was mutated to Phe149. Therefore, the roles of Asp137 and Tyr149 in the activity of the enzyme were postulated. It is noteworthy that the segment Ala122–Ser129, which is in the proximity of Tyr149, was not observed in the structure of HylP1. Accordingly, the effects of its interactions on Tyr149 could not be analysed. In the present structure of HylP2, the loop Ala122–Ser129 has been modelled satisfactorily in the electron density. The examination of this part of the structure shows that TyrB149 OH is at a distance of 3.1 Å from SerA129 O. SerA129 is part of the loop AlaA122–SerA129 and is also the central residue of a tight inverse γ-turn ($\varphi = -87$, $\psi = 41$) in which SerA128 O is hydrogen bonded to ThrA130 NH (O·NH = 3.0 Å). The additional intra-loop interactions include a hydrogen bond, and several hydrophobic interactions. A number of interactions have also been observed between the loop AlaA122–SerA129 and neighbouring protein residues, including AlaA121 NH·ThrC113 O, ThrA130 O·GlnC115 $N^{\varepsilon 2}$, GlyA131 O·GlnC115 $N^{\varepsilon 2}$ and GlyA132 O·GlnC115 $N^{\varepsilon 2}$. TyrB149·OH is involved in the interactions with AspC137 $O^{\delta 1}$ and AsnC135 $O^{\delta 1}$. As a result, Tyr149 appears to be a poor candidate for enzymatic catalysis. However, further studies with various substrate analogues and other longer ligands are required to establish the mechanism of ligand binding and product formation.

Ascorbic acid inhibits the functional activity of HylP2

Ascorbic acid has previously been shown to be a competitive inhibitor of hyaluronidases [12–14]. On the basis of this information, we performed an enzyme activity assay confirming that ascorbic acid inhibits the degradation of hyaluronan by HylP2. Under our experimental conditions, the IC_{50} of this inhibition was found to be approximately 1 mM.

The inhibition data of enzyme HylP2 with ascorbic acid, together with its chemical and structural similarities with hyaluronan polysaccharide, suggest that ascorbic acid may bind at the saccharide binding site. Therefore, it may act as a protective factor for the host tissue hyaluronan because these tissues are not degraded by the hyaluronate lyase in the presence of ascorbic acid. In host tissue matrix, the ascorbic acid exists at concentrations in the range 0.2–8 mM [15], which are within the range of the IC_{50} of ascorbic acid against HylP2. For the first time, the present study provides insight into the inhibitor binding sites in HylP2 and postulates the substrate binding regions in the bacteriophage enzyme as a result of ascorbic acid being structurally similar to the glucuronate residues in hyaluronan polysaccharide.

Ligand binding in HylP2

To define the binding surface with residues that are important in recognition, two complexes of HylP2 with ascorbic acid and lactose were prepared. As noted above, ascorbic acid was found to inhibit the activity of HylP2, whereas lactose was used as a substrate product analogue ligand. The crystals of the native protein were soaked in solutions containing ascorbic acid and lactose separately for 48 h and the crystal structures of the two complexes were determined and refined at resolutions of 3.1 and 2.6 Å respectively. The structures of the complexes revealed that both the ligands occupy three subsites on the three concave surfaces covering almost the full length of the TSβH domain. The protein residues that constitute the polysaccharide binding site belong to all three polypeptide chains (Tables 2 and 3). Although residues AspC137 and TyrB149 do not interact directly with these two ligands, they lie on the same side of the surface in close proximity to the interacting residues and were interacting with the actual substrate.

Ascorbic acid binding

Ascorbic acid (Fig. 1A) inhibits the activity of HylP2. The structure of the complex of HylP2 with ascorbic acid shows that three molecules of ascorbic acid bind to HylP2 trimer at each one of the three concave surfaces (Fig. 4). At site 1, ascorbic acid is involved in the interactions primarily with GluB167 and LysC179 (Table 2). GluB167 $O^{\varepsilon 2}$ interacts with ascorbic acid O2H with a hydrogen bond at a distance of 2.5 Å, whereas LysC179 N^{ζ} forms two bifurcated hydrogen bonds with the O1 and O4 atoms of ascorbic acid. It is interesting to note that the side chains of both

Table 2. Hydrogen bonded interactions between HylP2 and ascorbic acid at three binding regions in the polysaccharide binding groove.

Atoms of ascorbic acid	Protein/water atoms	Distance (Å)
Molecule 1		
O1	Lys C179 N^{ζ}	3.1
O2	Glu B167 $O^{\varepsilon 2}$	2.6
O4	Lys C179 N^{ζ}	2.5
Molecule 2		
O1	Gln C214 $N^{\varepsilon 2}$	2.5
O2	Arg C216 N^{ε}	3.3
O4	Asn B202 $N^{\delta 2}$	3.1
O6	Asn A183 $N^{\delta 2}$	2.7
Molecule 3		
O1	Gln C261 $N^{\varepsilon 2}$	3.2
O2	Asn B241 O	2.9
O3	W C1[a]	2.8
	W C1[a] → Ser B246 O^{γ}	3.3
	W C1[a] → Gly A223 N	2.8
O5	Tyr C264 OH	2.8
O6	Asn C266 $N^{\delta 2}$	3.2

[a] The water molecule forms a bridge between ascorbic acid atom and protein atoms.

GluB167 and LysC179 at this subsite undergo significant conformational changes upon binding to ascorbic acid (Fig. 2). The second molecule of ascorbic acid interacts with AsnA183, AsnB202, GlnC214 and ArgC216 (Table 2). At this subsite, the ascorbic acid molecule is buried in the protein, forming at least four hydrogen bonds. As a result of binding, the conformations of side chains of AsnA183 and AsnB202 remain unperturbed, whereas those of GlnC214 and ArgC216 undergo minor conformational changes (Fig. 2B). The third molecule of ascorbic acid interacts most extensively with the protein atoms (Table 2). The residues GlyA223, AsnB241, SerB246, GlnC261, TyrC264 and AsnC266 participate in the interactions with various atoms of the ascorbic acid and stabilize its binding at this site. However, by contrast to positions 1 and 2, the protein residues do not undergo appreciable conformational variation (Fig. 2C).

Lactose binding

As observed in the case of ascorbic acid, lactose (galactose 1β → 4 glucose) (Fig. 1B) also binds to the protein at three positions on the single substrate binding site of the triple assembly (Fig. 4A). The view from the top shows the lactose binding on three faces (Fig. 4B). Position 1 is observed near the β-strands, β4 and β5, and the interactions involve residues AspA151, GlyB165 and LysB166. At least six hydrogen bonds

Table 3. Hydrogen bonded interactions between HylP2 and lactose at three binding regions in the polysaccharide binding groove.

Atoms of lactose	Protein/water atoms	Distance (Å)
Molecule 1		
O1′	W A16	2.6
O2′	Gly B165 O	2.5
O3′	Gly B165 O	2.7
	Lys B166 N^{ζ}	2.8
O2	Lys B166 N^{ζ}	3.3
O6	Asp A151 $O^{\delta 2}$	2.9
Molecule 2		
O1′	Gln C214 $N^{\varepsilon 2}$	2.5
O2′	W C73[a]	2.9
	W A73[a] → W A103[a]	3.0
	W A103[a] → Thr A228 $O^{\gamma 1}$	2.8
	W A103[a] → Leu C215 O	3.0
O6′	W A101[a]	2.7
	W A101[a] → Phe B197 O	2.5
	Ser B198 O^{γ}	3.3
	Asn A183 $O^{\delta 1}$	3.3
O4	Asn A186 $N^{\delta 2}$	2.9
O6	Asn A186 $O^{\delta 1}$	3.0
	Thr B204 $O^{\gamma 1}$	3.2
Molecule 3		
O1′	Arg A277 NH2	2.5
O2′	Arg A279 NH1	3.3
	W A105	2.5
O6′	W A82	3.2
	Asn B241 $O^{\delta 1}$	3.0
	Arg A277 NH1	2.5
	Gln C261 $N^{\varepsilon 2}$	3.2
	Gln C261 $O^{\varepsilon 1}$	3.1
O1	Tyr C264 OH	3.2
O2	Asn B241 O	2.5
	Gln C261 $O^{\varepsilon 1}$	3.2
O4	Ser B246 O^{γ}	2.5
	W A110[a]	2.7
	W A110[a] → Ser B246 O^{γ}	3.1
	W A110[a] → Gly A223 N	3.2

[a] The water molecule forms a bridge between lactose atom and protein atoms.

have been observed between the protein and the ligand (Table 3). The second lactose molecule is held near β-strands β7, β8 and β9 (Table 3). At this position, lactose forms several hydrogen bonds involving various protein residues, AsnA183, AsnA186, PheB197, SerB198, ThrB204, GlnC214 and ThrA228, and water molecules, W73, W101 and W103. The third lactose molecule is located near the β-strands β11, β12 and β13 (Table 3). It interacts with GlyA223, AsnB241, GlnC261, TyrC264, ArgA277 and ArgA279. The water molecule W110 is also a part of the hydrogen bonded network formed between protein residues and lactose. Although the complexes of lactose with protein are involved in extensive interactions, the conformational

perturbations in the protein do not occur. The superimpositions of two complexes formed with ascorbic acid and lactose indicate that both ligands bind to protein almost at the same regions of the concave substrate binding sites (Fig. 4). In the case of position 1 only, ascorbic acid binds at a position that is approximately 4 Å away from that of lactose binding site. This is a result of the presence of AspA151 at the position of the lactose binding site, which does not create favourable conditions for the binding of ascorbic acid.

Catalytic site

The structures of native protein HylP2 and its complexes with ascorbic acid and lactose revealed the presence of three long concave surfaces on the triple-stranded β-helix domain. One of these surfaces containing the residues shown in Tables 2 and 3 indicates a typical saccharide binding environment [16]. The structures of the complexes further show that three molecules of each ascorbic acid and lactose are present at each of the three grooves on the protein surface. Mutation studies, together with observed interactions between the residues of HylP2 and the ligands, indicate that the catalytic site appears to be centred in the proximity of Tyr264 (Fig. 5). Indeed, the orientations and spacing of Gln261, Tyr264 and Arg279 (Fig. 5B) suggest that these three residues form the most appropriate combination for a catalytic role. The stereochemical arrangement indicates that Gln261 may act as a partial electron sink, whereas Arg279 acts as a base. At the same time, Tyr264 acts as an acid and donates hydrogen to the glycosidic oxygen, leading to the cleavage of the β-1,4 covalent glycosidic bond [16].

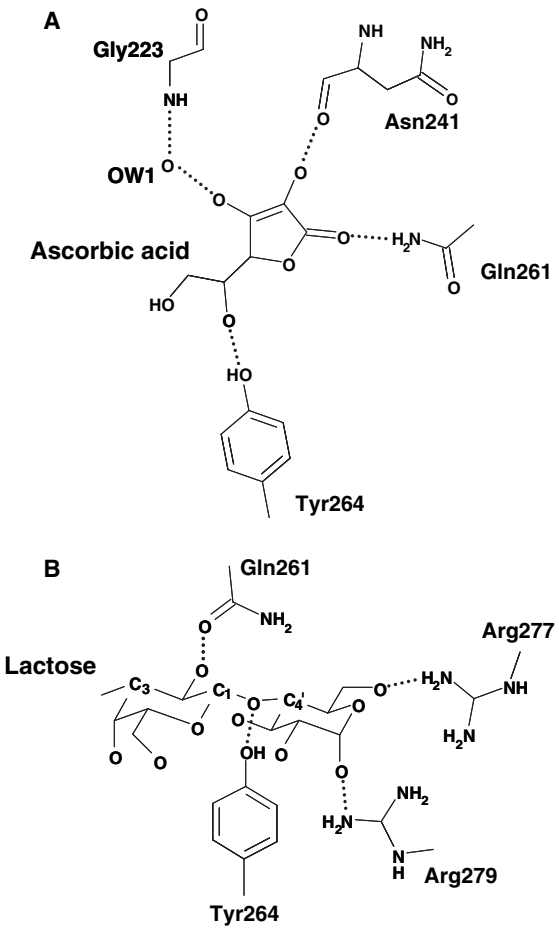

Fig. 5. Schematic diagram showing the interactions between the protein and ligand atoms at subsite 3 for (A) ascorbic acid and (B) lactose.

Discussion

We have not yet obtained the crystals of HylP2 complex with the HA substrate or its analogue. However, with the help of the structures of the native protein and its two complexes with ascorbic acid and lactose, we were able to obtain insight into the regions that are critical for ligand binding. The substrate of this enzyme is a polysaccharide consisting of repeating units of 2-acetamino-2-deoxy-β-D-glucose and β-D-glucuronic acid, which is highly negatively charged because the pK_a of the glucuronic acid moiety in the substrate is approximately 3.2 [17]. Hence, the positive charges in the groove will be essential for attachment in the substrate binding site of the HylP2 molecule for the negatively charged substrate molecules.

The concave substrate binding site of HylP2 is of approximately 60 Å long. Its binding surface consists of predominantly charged and polar residues, which are distributed in patches. There are three major sites of concentration, with a spacing of 11 Å between subsites 1 and 2 and 14 Å between subsites 2 and 3, respectively. The first molecule of ascorbic acid is held at the lower-most subsite consisting of residues LysC179 and GluB167. LysC179 forms two hydrogen bonds involving O1 and O4 atoms of ascorbic acid, whereas GluB167 $O^{\varepsilon 2}$ interacts with ascorbic acid via O2H. This site is specific for the binding because of the unique positions of LysC179 and GluB167 and the scope of conformational changes of their side chains (Fig. 2A). On moving further from the N-terminus and towards the C-terminus, there is another cluster of residues consisting of GlnC214, ArgC216, AsnB202 and AsnA183, where a second molecule of ascorbic acid is held firmly. As shown in Fig. 2B, the hydrogen bond acceptors O2, O1, O4 and O6 from one side of ascorbic acid interact with ArgC216 N^{ε}, GlnC214 $N^{\varepsilon 2}$, AsnB202 $N^{\delta 2}$ and

AsnA183 $N^{\delta 2}$ and hold ascorbic acid firmly at this position. On moving further in the same direction, another potential subsite consisting of residues GlyA223, AsnB241, SerB246, GlnC261, TyrC264 and AsnC266 is present. As shown in Fig. 2C, four out of six oxygen atoms are involved in the interactions with protein/water atoms. This is one of the most firmly held ascorbic acid molecules, indicating the strong nature of the binding of ascorbic acid to proteins. Although ascorbic acid is a small molecule, it blocks the most attractive binding subsites in the protein, leading to the inhibition of the enzyme action.

Similarly, three molecules of lactose also bind in an almost identical manner and with subsites similar to those of ascorbic acid. The first molecule of lactose interacts with AspA151, GlyB165 and LysB166 and forms at least six hydrogen bonds and several van der Waals interactions. Most of these distances (Table 3) are less than 3 Å in length, indicating tight binding. Lactose is a product that has excellent complementarity. It is noteworthy that the interacting residues in lactose are slightly different from those observed in the first position with ascorbic acid. Although both are in close proximity, the binding position is not compatible to ascorbic acid as a result of the unfavourable orientation of the side chain of AspA151. The second lactose binding site involves residues AsnA183, AsnA186 and GlnC214 (Table 3). As shown in Fig. 3B, lactose oxygen atoms O4, O6, O1, O6′ and O1′ are aligned to interact with protein atoms. The third position of lactose binding consists of residues, TyrC264, GlnC261, ArgA277, ArgA279 and AsnB241. As shown in Fig. 3C and Table 3, this subsite also generates a number of interactions, including hydrogen bonds and van der Waals forces. The subsite appears to be involved in the catalytic activity because residues Gln261, Tyr264 and Arg279 provide a favourable stereochemical environment. The enzyme did not show activity when Tyr264 was mutated to Phe264. These binding sites with lactose clearly indicate the complementarity of the protein concave binding surface to a disaccharide product such as lactose.

Both ascorbic acid and lactose occupy three subsites at the long polysaccharide binding site. However, it is intriguing to observe long blank spaces of 11 Å in length and 14 Å in length between subsites 1 and 2 and 2 and 3, respectively. An examination of these regions indicates that PheC175 protrudes into the substrate binding area between subsites 1 and 2. Thus, it hampers the attachment of ligand at this subsite. Similarly, the space between subsites 2 and 3 is occupied by hydrophobic residues LeuA222 and PheB197. Even though substrate anchoring residues are also present in the vicinity, the ligands are unable to bind because of steric factors that are a result of the hydrophobic residues. It suggests that the polysaccharide substrate is anchored at three regions that can be identified by ligand binding and are loosely held in the middle regions. This would help the product to be easily dissociated.

Conclusions

The structure of hyaluronate lyase HylP2 is essentially similar to the structure of hyaluronate lyase HylP1. In HylP1, residues Asp137 and Tyr149 were predicted to comprise part of the active site and a loop Ala122–Ser129 was not observed in the structure because it was considered to be disordered. In the structure of HylP2, the loop Ala122–Ser129 is observed and it appears that it has a stable conformation with a number of interactions within the loop, as well as with other parts of the protein. It is important to note that Ser129 interacts with Tyr149, thus making it inaccessible for interactions with the polysaccharide substrate, indicating that the residue Tyr149 may not be involved in the catalysis. On the other hand, Tyr264 is fully exposed and is involved in the interactions with ascorbic acid, as well as with lactose, indicating its suitability for a catalytic role. Its positioning together with Gln261 and Arg277 with respect to the lactose molecule suggests a functional role for Tyr264. Furthermore, kinetic studies indicate a loss of activity when Tyr264 is mutated to Phe264. The structures of the complexes of HylP2 indicate the existence of three subsites in the long concave binding site of the enzyme where lactose and ascorbic acid are located. The binding characteristics of these subsites can be exploited for the design of inhibitors of HylP2.

Experimental procedures

Cloning, expression, and purification

The full-length gene for HylP2 of 1014 nucleotides was cloned into pET21d (+) vector with *Nhe*I and *Xho*I restriction sites. Recombinant HylP2 containing a C-terminal His6 tag was over-expressed in *Escherichia coli* BL21 expression cells and purified in its enzymatically active form by Ni^{2+} chelate chromatography and size exclusion chromatography, as described previously [6]. The size exclusion chromatography and glutaraldehyde cross-linking experiments suggested the existence of a catalytically active HylP2 trimer. The complete nucleotide and deduced amino acid sequences are available in the sequence data base with accession number AAA86895.

Activity assay

The *in vitro* activity assay for HylP2 was performed using HA as substrate and ascorbic acid as an inhibitor. The activity of the enzyme was determined by measuring its ability to breakdown HA to unsaturated disaccharide units [18]. One millilitre of solution with increasing concentrations of ascorbic acid was added to buffer containing 50 mM sodium acetate, 20 mM calcium chloride (pH 6.0) and 2 μg of full-length native HylP2 at pH 7.0 (diluted just before taking the measurement) and incubated at 4 °C for 3 h. Then 0.3 $mg{\cdot}mL^{-1}$ HA was added to the reaction mixture just before taking the reading. The kinetic parameters were calculated using an extinction coefficient of $5.5 \times 10^{-3}{\cdot}M^{-1}$ for the disaccharide products.

Crystallization

The purified HylP2 was dissolved in 10 mM Hepes, 100 mM NaCl, pH 7.2, to a final concentration of 10 $mg{\cdot}mL^{-1}$. The protein was crystallized using the sitting drop vapour diffusion method at 293 °K in 24-well Linbro plates (ICN Biomedical Division, Carson, CA, USA). Droplets containing a mixture of 5 μL of protein solution and 5 μL of reservoir solution were equilibrated against the reservoir containing 3.25 M sodium formate. The crystals of native protein were soaked in the two sets of reservoir solutions containing ascorbic acid and lactose separately at a concentration of 100 $mg{\cdot}mL^{-1}$. The crystals of the complexes were prepared by soaking the crystals of native protein in the reservoir solutions containing ascorbic acid and lactose at a concentration of 100 $mg{\cdot}mL^{-1}$ for 48 h.

Detection of ascorbic acid in crystals

Ascorbic acid detection was carried out using the solution of an organic compound 2,6-dichlorophenolindophenol [19]. The test solution was added dropwise to 2.5 mL of the indicator solution until the blue colour of the solution cleared, indicating the presence of ascorbic acid.

Detection of lactose in crystals

To confirm the presence of lactose in the crystals, the crystals were picked up from the crystallization plates, washed thoroughly with reservoir solution and then dissolved in triple distilled water. NaCl was added to the protein solution. It was ultrafiltered using a 1 kDa cut-off membrane. The ultrafiltered samples were lyophilized and dissolved in water at a concentration in excess of than 0.5 $mg{\cdot}mL^{-1}$. Benedict's reagent [20], consisting of sodium bicarbonate, sodium citrate and copper sulfate, was added to this solution. The solution was heated on a water bath and the change of colour indicated the presence of lactose in solution.

X-ray intensity data collection

The crystals of HylP2 were transferred into reservoir solution containing 35% methanepentandiol as a cryo-protectant for data collection at 100 °K. The X-ray intensity data were collected using synchrotron beam line X13 radiation, at DESY (Hamburg, Germany), with a wavelength of 0.803 Å using a MAR345 imaging plate scanner (Marresearch GmbH, Norderstedt, Germany). All three data sets were processed and scaled using DENZO and SCALEPACK software [21]. The data collection and data processing statistics for the three data sets are provided in Table 1.

Structure determination and refinement

The structure was determined with molecular replacement method using AMORE [22] from the CCP4 software suite [23]. The coordinates of hyaluronidase HylP1, which has a sequence identity of more than 90% (Protein Data Bank code: 2C3F) [5], were used as the search model. Both rotation and translation searches resulted in unique solutions that were well above the noise levels. Further positional and B-factor refinements were performed using the REFMAC5 software suite [24]. The refinement calculations were interleaved with several rounds of model building with the software O [25]. The omit maps were calculated for segments Ala122–Ser129 and Gln191–Ser199 and the protein chains were adjusted into electron densities with a lower cut-off (0.7 σ) (Fig. 6). The difference electron density $|F_o - F_c|$ maps computed when R_{cryst} was 0.264 for the two data sets obtained from soaked crystals indicated extra electron densities at three sites on each face of the triple-stranded assembly. The ascorbic acid and lactose molecules were modelled into these electron densities as shown in Figs 2 and 3, respectively. These were also included in further cycles of refinements. Numerous water molecules were also clearly visible in the difference Fourier maps. They were easily picked and were added to the subsequent refinement cycles. Several further rounds of refinement with REFMAC5 [23] interspersed with model building using $|2F_o - F_c|$ and $|F_o - F_c|$ Fourier maps converged the refinement to R_{cryst} (R_{free}) factors of 0.191 (0.219), 0.197 (0.233) and 0.191 (0.226) for the structures of native protein and its complexes with ascorbic acid and lactose, respectively. The positions of only those water molecules were retained in the final model if they met the criteria of peaks greater than 2.5 σ in the final $|2F_o - F_c|$ maps, had hydrogen bond partners at appropriate distances with proper angle geometry, and the B-factor values were less than 75 $Å^2$ in the final refinement cycle. A summary of the refinement statistics is provided in Table 1.

The atomic coordinates for the refined structures of native HylP2 and its complexes with ascorbic acid and lactose have been deposited in the Protein Data Bank with accession codes 2YW0, 3EKA and 2YVV, respectively.

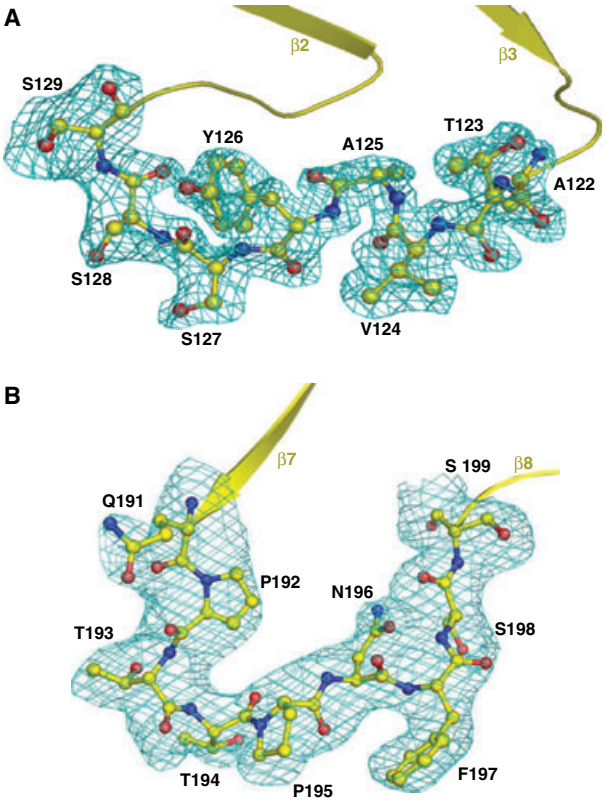

Fig. 6. Fourier ($|2F_o - F_c|$) map calculated by omitting segments (A) Ala122–Ser129 and (B) Gln191–Ser199 at a cut-off of 1 σ.

Acknowledgements

The authors acknowledge financial support from the Department of Biotechnology (DBT), New Delhi. Parul Mishra, R. Prem Kumar and Abdul Samath Ethayathulla thank the Council of Scientific and Industrial Research (CSIR), New Delhi for the award of fellowships. Tej P. Singh is grateful to the Department of Biotechnology (DBT), New Delhi for the award of Distinguished Biotechnologist.

References

1 Meyer K (1971) Hyaluronidases. In *The Enzymes* (Boyer PD, ed), Vol. 3, pp 307–320. Academic Press, NY.
2 Kreil G (1995) Hyaluronidases – a group of neglected enzymes. *Protein Sci* **4**, 1666–1669.
3 Niemann H, Birch-Anderson A, Kjems E, Mansa B & Stirm S (1976) Streptococcal bacteriophage 12/12 borne hyaluronidase and its characterization as a lyase (EC 4.2.99.1) by means of streptococcal hyaluronic acid and purified bacteriophage suspensions. *Acta Pathol Microbiol Scand Sect B* **84**, 145–153.
4 Hynes WL, Hancock L & Ferretti JJ (1995) Analysis of a second bacteriophage hyaluronidase gene from *Streptococcus pyogenes*: evidence for a third hyaluronidase involved in extracellular enzymatic activity. *Infect Immun* **63**, 3015–3020.
5 Smith NL, Taylor EJ, Lindsay A, Charnock SJ, Turkenburg JP, Dodson EJ, Davies GJ & Black GW (2005) Structure of a group A streptococcal phage-encoded virulence factor reveals a catalytically active triple-stranded β-helix. *Proc Natl Acad Sci USA* **102**, 17652–17657.
6 Mishra P, Akhtar MS & Bhakuni V (2006) Unusual structural properties of bacteriophage associated hyaluronidase (HylP2). *J Biol Chem* **281**, 7143–7150.
7 Baker JR, Dong S & Pritchard DG (2002) The hyaluronan lyase of *Streptococcus pyogenes* bacteriophage H4489A. *Biochem J* **365**, 317–322.
8 Broudy TB, Pancholi V & Fischetti VA (2001) Induction of lysogenic bacteriophage and phage-associated toxin from group A streptococci during coculture with human pharyngeal cells. *Infect Immun* **69**, 1440–1443.
9 DeLano WL (2002) *The PyMOL Molecular Graphics System*. DeLano Scientific, San Carlos, CA.
10 Ramachandran GN & Sasisekharan V (1968) Conformation of polypeptides and proteins. *Adv Protein Chem* **23**, 283–438.
11 Laskowski RA, MacArthur MW, Moss DS & Thornton JM (1993) PROCHECK: a program to check the stereochemical quality of protein structures. *J Appl Crystallogr* **26**, 283–291.
12 Menzel EJ & Farr C (1998) Hyaluronidase and its substrate hyaluronan: biochemistry, biological activities and therapeutic uses. *Cancer Lett* **131**, 3–11.
13 Li S, Taylor KB, Kelly SJ & Jedrzejas MJ (2001) Vitamin C inhibits the enzymatic activity of *Streptococcus pneumoniae* hyaluronate lyase. *J Biol Chem* **276**, 15125–15130.
14 Botzki A, Rigden DJ, Braun S, Nukui M, Salmen S, Hoechstetter J, Bernhardt G, Dove S, Jedrzejas MJ & Buschauer A (2004) L-ascorbic acid 6-hexadecanoate, a potent hyaluronidase inhibitor: x-ray structure and molecular modeling of enzyme-inhibitor complexes. *J Biol Chem* **279**, 45990–45997.
15 Bergsten P, Amitai G, Kehrl J, Dhariwal KR, Klein HG & Levine M (1990) Millimolar concentrations of ascorbic acid in purified human mononuclear leukocytes Depletion and reaccumulation. *J Biol Chem* **265**, 2584–2587.
16 Jedrzejas MJ, Mello LV, de Groot BL & Li S (2002) Mechanism of hyaluronan degradation by *Streptococcus pneumoniae* hyaluronate lyase Structures of complexes with the substrate. *J Biol Chem* **277**, 28287–28297.
17 Cleland RL, Stoolmiller AC, Rodén L & Laurent TC (1969) Partial characterization of reaction products formed by the degradation of hyaluronic

acid with ascorbic acid. *Biochim Biophys Acta* **192**, 385–394.
18 Pritchard DG, Lin B, Willingham TR & Baker JR (1994) Characterization of the group B streptococcal hyaluronate lyase. *Arch Biochem Biophys* **315**, 431–437.
19 VanderJagt DJ, Garry PJ & Hunt WC (1986) Ascorbate in plasma as measured by liquid chromatography and by dichlorophenolindophenol colorimetry. *Clin Chem* **32**, 1004–1006.
20 Benedict SR (1908) A reagent for the detection of reducing sugars. *J Biol Chem* **5**, 485–487.
21 Otwinowski Z & Minor W (1997) Processing of X-ray diffraction data collection in oscillation mode. *Methods Enzymol* **276**, 307–326.
22 Navaza J (1994) *AMoRe*: an automated package for molecular replacement. *Acta Crystallogr A* **50**, 157–163.
23 Collaborative Computational Project, Number 4 (1994) The CCP4 suite: programs for protein crystallography. *Acta Crystallogr D* **50**, 760–763.
24 Murshudov GN, Vagin AA & Dodson EJ (1997) Refinement of macromolecular structures by the maximum-likelihood method. *Acta Crystallogr D* **53**, 240–255.
25 Jones TA, Zou JY, Cowan SW & Kjeldgaard M (1991) Improved methods for building protein models in electron density maps and the location of errors in these models. *Acta Crystallogr A* **47**, 110–119.